SPEKTA
(Jurnal Pengabdian Kepada Masyarakat: Teknologi dan Aplikasi)
ISSN 2723-8016 (online) | 2723-8008 (print)
Vol 5, No. 1, pp. 60-72

Experiment Evaluation on the Porosity of Plasma Coating from Ceramic Al_2O_3 – TiO_2 Using the Metallography

Vu Duong [a], Ha Minh Hung [b]

[a] School of Engineering and Technology, Duy Tan University, Da Nang, 550000, Vietnam
[b] National Research Institute of Mechanical Engineering, Hanoi, Vietnam
* Corresponding Author: duongvuaustralia@gmail.com

ARTICLE INFO

Article history
Received October 22, 2023
Revised February 17, 2024
Accepted April 2, 20024

Keywords
Plasma spray,
ceramic material;
Al_2O_3 – TiO_2;
design experiment;
metallographic porosity

ABSTRACT

Background: The objective of this paper is an experimental investigation of the metallographic porosity of plasma coating using standard materials from the ceramic system Al_2O_3-TiO_2 on the substrate of steel SS400 at laboratory scale Lab at the Research Institute of Mechanical Engineering.
Contribution: The main contribution of the research is the evaluation of the porosity of the coating under the influence of the main technological parameters since the porosity plays a significant role in the performance of the working surface using the built-in Image Pro-Analyzer software in the Axiovert 25 MAT microscope.
Method: The spraying material is Al_2O_3-TiO_2 powder. The input parameters are: spraying distance (Lp; current of plasma stream (Ip); powder feed flow (Gp and spraying rate (Vp).
Results: The findings show that the average porosity of the Al_2O_3-TiO_2 plasma coating is inversely decreasing in the increasing direction of the distance: spray in the range Lp = 100–200 mm, increase proportional to the increase of the current plasma flow rate in the range Ip = 400–600 A, provided that the powder feed flow Gp = 1.7 kg/h and the spraying rate Vp = 50 mm/min.
Conclusion: The degree of influence of the three main technological parameters (Lp, Ip, and Gp) in the survey limit domain may be due to the selected Lp spray distance within the relatively wide recommended range of the plasma spraying equipment supplier. It is recommended to conduct the experimental planning of the L27 type to localize the optimum area.

1. Introduction

In industrialized countries around the world, thermal coating technology, including plasma spraying, has been researched and applied to create ceramic coatings such as Al2O3

+ ZrO2 [1] and Al_2O_3 + TiO_2 with TiO_2 content varying at 3 levels of 3%, 13%, and 40% TiO2 [2, 3, 4, 5]. In every study mentioned above, the content focused on different issues. For example, in [2], the comparison between the flame and plasma sparying is according to the porosity, but the sparying material is not the same. Namely, the porosity in flame spraying is slightly lower than in plasma spraying due to the flexible core material. At the same time, the input parameters, such as the feeding rate, the plasma current, and the fuel pressure, are not changing. The effect of the laser remelting on the microstructure and erosion resistance was evaluated using the intensive mode of plasma spraying: plasma power of 80 kW, current of plasma of 1000 A, and powder feed rate of 100 g/min [3, 4]. In [5], the comparison between nitrogen and argon as plasma generation gases was made when the nanostructure featuring the level of melting was focused. The analysis shows the advantage of nitrogen over argon as the essential plasma gas. The thermophysical properties of the ethylene glycol-based TiO2 + Al2O3 hybrid nanofluid are the specific feature in [6]. The melting level of the coating was improved since the thermal conductivity and the viscosity of the feeding stock positively affected the temperature concentration. There are different ways to produce the spraying material, even with the same proportion.

The distinghable effect of spraying was demonstrated in [7], namely that the crushed and fused powder is better than the simlpe blending mixture. The deep investigation on the tribology properties of the plasma-sprayed coatings with the different content of TiO2 (3%, 13%, and 40%, respectively) was conducted in [8]. They observed that the elevated content of TiO2 decreased the hardness of the coating, and the wear resistance was influenced by not only the decreased hardness due to the increased TiO2 content but also different phase compositions in the coating.In the experiment with the different content of TiO2 in the composition with Al2O3, the researchers refer to the regulations of standards [9,10,11].The Al2O3 + 13% TiO2 plasma coating sprayed on the application part through the NiCrAl intermediate technology liner has clarified pores and bridges between sprays and increased its anti-rust performance, better protecting the spray part [12].

The only feature is the evaluation of the sealing effect using silicon after deposition. The new progress was observed in [13], when the aim of the work focused on the performance of the coating Al2O3 + 13% TiO2 under the influence of two parameters, such as the spray distance and the torch linear velocity. It is noted that the wear resistance of the coating increased significantly with the decreased spraying distance since the feedstock particles were better melted and the microstructure of the layer was improved. But the question about the influence of the plasma power on the microstructure of the coating needs to be clarified. In this regard, another study [14] introduced the experiment observing the influence of the heat flux, power input, flow rate of argon, and spray distance on the wear resistance of the coating. But the composition of the feedstock is Al2O3 + 3% TiO2. Here, the indirect relationship between the heat flux and the torch linear velocity was explained.

The earlier publication [15] showed a very detailed influence of the separate input parameters of the plasma spying composition of Al2O3 and 3% TiO2 on the wear resistance and adhesion of the coating. The lack of simultaneous evaluation of the main input parameters encourages the author to start a new investigation. The specific novelty of the coming experiment is also the use of ordinary air as the plasma generation gas to save on production costs [16]. From this analysis, the simultaneous influence of some main plasma

input parameters is not enough studied to regulate the technological procedure in terms of localization of the optimum area.

Up to now, in Vietnam, there have been a number of studies on the application of thermal spraying technology deployed from 2012 to now at the Mechanical Research Institute (Ministry of Industry and Trade) on $Ni_{18}Cr_5Al_4B$ plasma coating on the surface of mechanical wear-resistant carbon steel. The Institute of Tropical Technology (Vietnam Academy of Science and Technology) focused on $NiCr_5Al$ double coating against chemical corrosion by electric arc spraying technology. Hanoi University of Industry investigated plasma coating to protect carbon steel surfaces. But all these experiments were only done at the laboratory scale and tested on single mechanical products according to the requirements of recovery after wear and damage.

The aim of this work is to fill the existing gap and continue the experience gained during the setting of a collaboration program to improve the performance of the Al2O3+ TiO2 ceramic plasma sprayed. In this work, the research team introduces experimental results investigating the influence of some plasma spraying modes to create an Al2O3-TiO2 ceramic coating (using a standard powder with a content of 30% TiO2) on the metal porosity in the state after spraying to predict its working capacity.

2. Method

2.1. Problem statement

The samples after spraying are shaped like a 50 x 50 mm square and a round disc (50 mm), cut into small samples with a length of about (25 - 30 mm). The sampling location is selected at three different characteristic zones to be surveyed, including the center and different sub-zones, at a distance of (10 - 20 mm) from the center. The small samples received are then treated with the entire surface according to the cross-section of SS400 base steel and Al_2O_3-TiO_2 plasma coating.

The equipment SG-100 from Praxair Tafa (USA) used for the conduction of the plasma spraying in an open atmosphere. The polishing, cleaning, and culinating are carried out in accordance with the procedures of the Laboratory of Metallurgy and Heat Treatment of Hanoi University of Science and Technology Figure 1 Survey research and imaging of micromaterial cell organization are then carried out in selected characteristic structural subregions, including the Al_2O_3-TiO_2 plasma coating, the SS400 substrate steel layer, and the border between those two layers on the Axiovert 25 MAT optical microscope. The porosity of the coatings was determined using a special built-in software installed in the microscope.

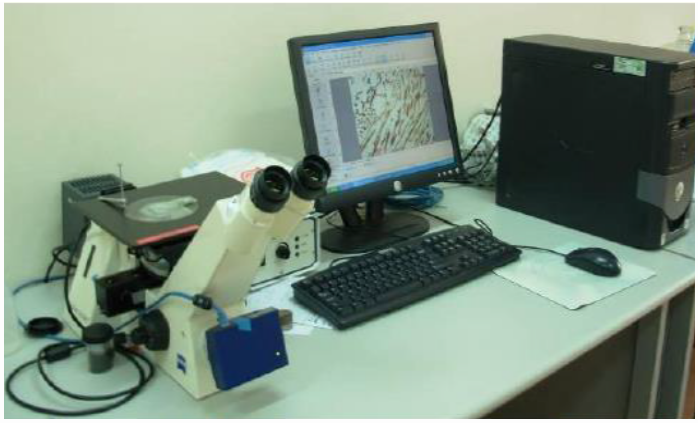

Figure 1. Axiovert 25 MAT optical microscope image

3. Result and Discussion

Experimental survey results on nine samples of orthogonal experimental planning type L9 are given in Table 1. Microscopic organization and porosity analysis of coating materials are given in Figures 2 and 3. Al_2O_3-TiO_2 plasma coating spray mode on the SS400 substrate steel surface selected here is conducted to study and investigate the simultaneous influence of all 3 input technology parameters, including injection distance (Lp), plasma current strength (Ip), and powder feed flow (Gp), on the output target function, which is the porosity determined by the needle plasmament method (p) when the injection speed parameter is selected at a fixed level (Vp = 60 mm/s).

Table 1. Metallic porosity of plasma coating materials Al2O3 – TiO2

No	Code	L, mm	I, A	G, kg/h	Overage porosity of plasma coating Al2O3 – TiO2, %		
					Experiment	Simulation	Relative deviation
1	000	100	400	1,7	14,520	14,675	1,07%
2	010	100	500	1,7	13,538	12,88	-4,86%
3	020	100	600	1,7	11,355	11,125	-2,02%
4	100	150	400	1,7	10,985	11,159	1,59%
5	110	150	500	1,7	9,695	10,111	4,29%
6	120	150	600	1,7	7,765	8,8491	13,96%
7	200	200	400	1,7	8,125	8,2424	1,44%
8	210	200	500	1,7	7,773	7,6868	-1,11%
9	220	200	600	1,7	7,321	6,9176	-5,51%

Sample No. 1 (code 000) received when spraying with 3 main input technological parameters selected at the lowest level in the experimental planning domain: Lp = 100 mm, Ip = 400 A, and Gp = 1.7 kg/h, have plasma coating porosity values (p1 = 14.52%). Applying the smallest squared method to process empirical mathematical statistics for an L9-type orthogonal planning array resulted in a calculated simulation average porosity of 14.675%. The error between experimental values and simulation calculations is very small (+1.07%). A preliminary assessment of the entire ceramic coating surface shows that there is uniform alignment throughout the length of the sample. Microscopic organization and structural analysis of coating materials are given in Figure 2. a, and b.

The spraying mode for sample No. 2 (code 010) was selected with the adjustment of the plasma flow intensity parameter to the average in the experimental planning domain: Lp = 100 mm; Ip = 500 A; and Gp = 1.7 kg/h. In this experimental mode, Al_2O_3-TiO_2 plasma coating with relatively good bonding with SS400 base steel is ensured. The average porosity of the coating has a value of p2 = 13.538%, a decrease of 6.76% compared to sample No. 1 above. The porosity calculated according to the regression function model has a value of 12.888%. The error between the empirical values and the simulation calculations was very small (4.87%). The bonding between the ceramic coating and the base steel layer is fairly uniform over the entire length of the surveyed sample. Microscopic organization and structural analysis of coating materials are given in Figure 2. c, and d.

The porosity of test sample No. 3 (code 020), received in the plasma flow-adjusted injection mode, is highest in the experimental planning domain (Ip = 600 A), while the two parameters Lp = 100 mm and Gp = 1.7 kg/h remain low. The average porosity of the coating material has a value of p3 = 11.355%; a decrease of 14.99% is very significant compared to sample No. 2 considered above. The porosity calculated according to the regression function model has a value of 11.125%. The error between the empirical values and the simulation calculations is quite small (2.02%). The ceramic coating has good bonding over the entire length of the survey sample. Microscopic organization and structural analysis of coating materials are given in Figure 2. e, and f.

Experimental sample No. 4 (code 100) was received in spray mode in the experimental planning domain with: Lp = 150 mm; Ip = 400 A; and Gp = 1.7 kg/h. Here the injection distance is adjusted to medium, while Ip and Gp remain low in the experimental planning domain. The porosity of the Al_2O_3-TiO_2 plasma coating material in this experiment had an average value of p4 = 10.985%, down 3.258% compared to the two samples 3 above. The porosity calculated by the regression function model has a value of 11.159%. The error between experimental values and simulation calculations is quite small (+1.59%). According to the survey sample length, the ceramic coating has a good bond with the base steel layer. Microscopic organization and structural analysis of coating materials for Figure 2. g, and h.

The spray mode for sample No. 5 (code 110) was selected with adjustment of the spray interval parameter and plasma flow intensity to the average level in the experimental planning domain: Lp = 150 mm; Ip = 500 A, while ministerial traffic remains low in the experimental planning domain (Gp = 1.7 kg/h). The Al_2O_3-TiO_2 plasma coating has an average porosity of p5 = 9.695%, down 11.74% compared to sample 4 above. The simulated

calculated porosity has a value of 10.11%. The error between experimental values and simulation calculations is very small (+4.29%). The link between the two ceramic coatings and the base steel is quite good for the entire length of the sample. Microscopic organization and structural analysis of coating materials are given in Figure 2. k, and l.

Experimental sample No. 6 (code 120) was received in spray mode in the experimental planning domain with: Lp = 150 mm; Ip = 600 A; and Gp = 1.7 kg/h. Here the spray distance is adjusted to medium, while Ip and Gp remain low in the experimental planning domain. The porosity of the Al_2O_3 – TiO_2 plasma coating material in this experiment had an average value of p6 = 7.765%, a sharp decrease of 19.36% compared to the two samples 5 above. The porosity calculated by the regression function model has a value of 8.849%. The error between experimental values and simulation calculations is quite large (+13.96%). According to the survey sample length, the ceramic coating has a good bond with the base steel layer. Microscopic organization and structural analysis of coating materials are given in Figure 3. a, and b.

The porosity of test sample No. 7 (code 200), received in the plasma flow-adjusted injection mode, is highest in the experimental planning domain (Ip = 400 A), while the two parameters Lp = 200 mm and Gp = 1.7 kg/h are selected at a low level. The average porosity of the coating material has a value of p7 = 8.125%; a decrease of 14.99% is very significant compared to sample No. 2 considered above. The porosity calculated according to the regression function model has a value of 7.6868%. The error between experimental values and simulation calculations is quite small (1.11%). The ceramic coating has good bonding over the entire length of the survey sample. Microscopic organization and structural analysis of coating materials are given in Figure 3. c, and d.

Experimental sample No. 8 (code 210) was received in spray mode in the experimental planning domain with: Lp = 200 mm; Ip = 500 A; and Gp = 1.7 kg/h. Here the spray distance is adjusted to medium, while Ip and Gp remain low in the experimental planning domain. The porosity of the Al_2O_3 – TiO_2 plasma coating material in this experiment had a mean value of p8 = 7.773%, down 3.258% compared to the two samples No. 3 mentioned above. The porosity calculated by the regression function model has a value of 11.159%. The error between experimental values and simulation calculations is quite small (+1.59%). According to the survey sample length, the ceramic coating has a good bond with the base steel layer. Microscopic organization and structural analysis of coating materials are given in Figure 3. e, and f.

The spray mode for sample No. 9 (code 220) was selected with the parameter adjustment of the spray interval and plasma flow intensity to the highest level in the experimental planning domain: Lp = 200 mm; Ip = 600 A, while ministerial flow remains low in the experimental planning domain (Gp = 1.7 kg/h). The Al_2O_3 – TiO_2 plasma coating has an average porosity of p9 = 7.321%, down 5.81% compared to sample 8 above. The simulated calculated porosity has a value of 6.917%. The error between the empirical values and the simulation calculation is 5.51%. The link between the two ceramic coatings and the base steel is quite good for the entire length of the sample. Microscopic organization and structural analysis of coating materials are given in Figure 3. g, and h.

All 9 test samples considered above, the impact of injection distance (Lp) ensures the impact kinetic energy of $Al_2O_3 – TiO_2$ spray particles, plasma flow strength (Ip) and powder feed flow (Gp) all ensure the spray requirements necessary to create a coating with relatively good bonding with SS400 base steel. The average porosity of $Al_2O_3 – TiO_2$ plasma coating materials tends to decrease inversely proportionally to the increase of Lp parameters; Ip (when considering the boundary condition that Gp and Vp choose at a constant fixed level).

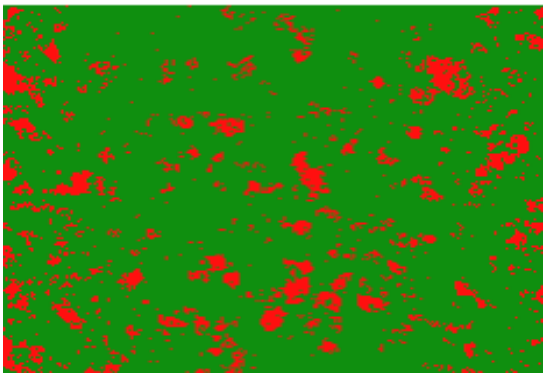

a) Sample 1 (MS: 000), x200

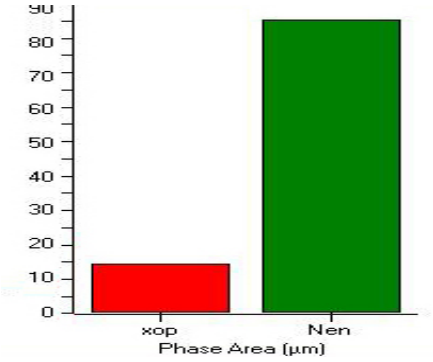

b) $\gamma_{p1} = 14{,}52$ %

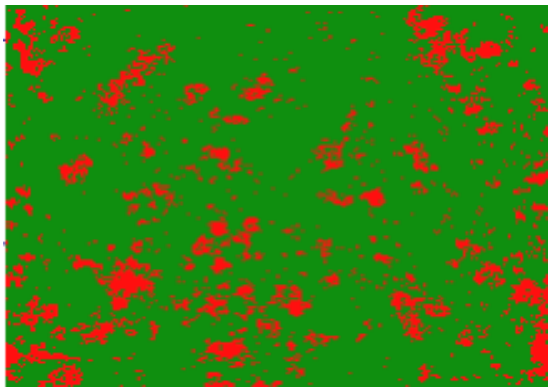

c) Sample 2 (MS: 010), x200

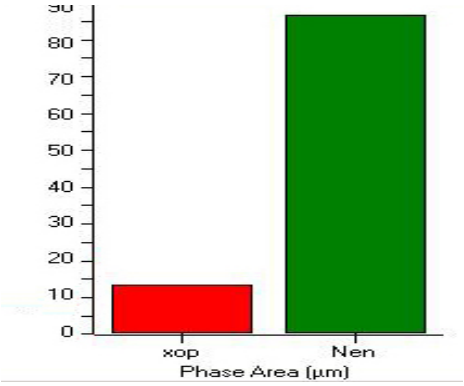

d) $\gamma_{p2} = 13{,}538$ %

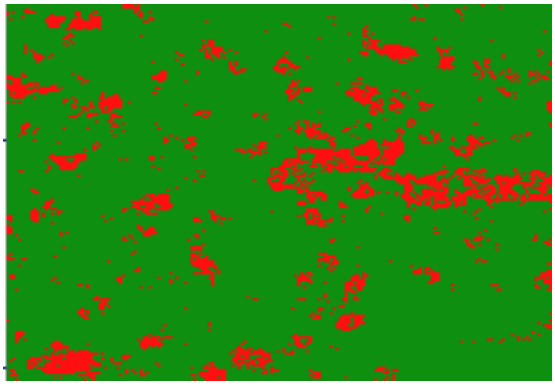

e) Sample 3 (MS: 020), x200

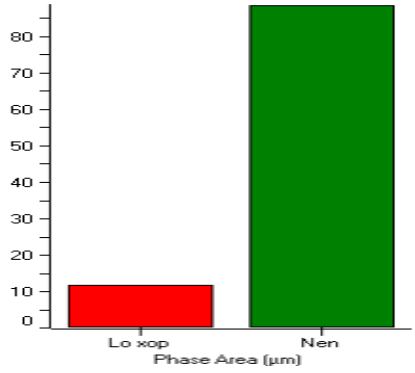

f) $\gamma_{p3} = 11{,}355$ %

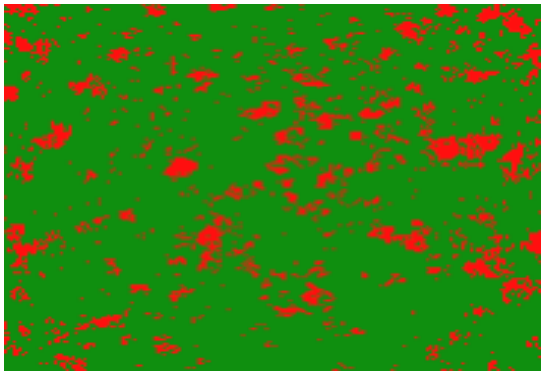

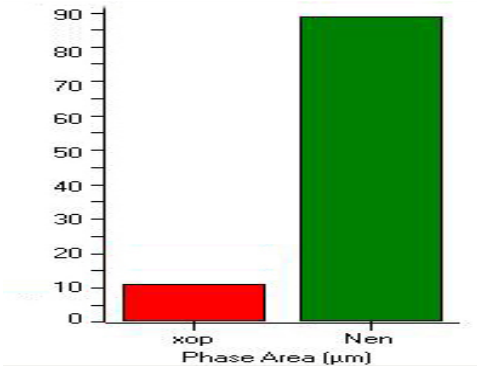

g) Sample 4 (MS: 020), x200

h) γ_{p4} = 10,985 %

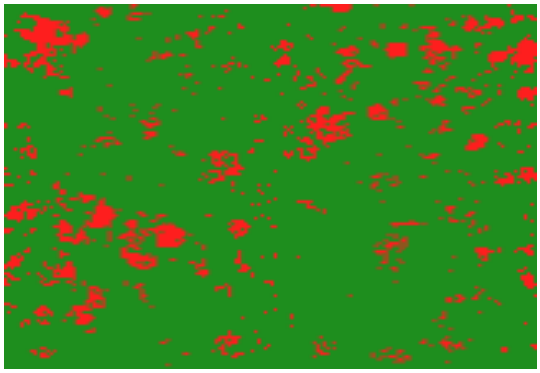

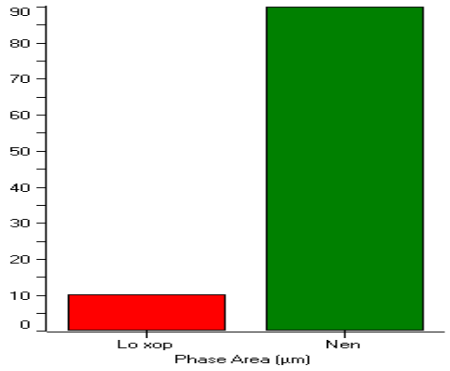

k) Sample 5 (MS: 020), x200

l) γ_{p5} = 9,695 %

Figure 2. Image of microstructure (a) and plasma coating porosity chart Al_2O_3 – TiO_2 (b) depends on Lp; Ip and Gp

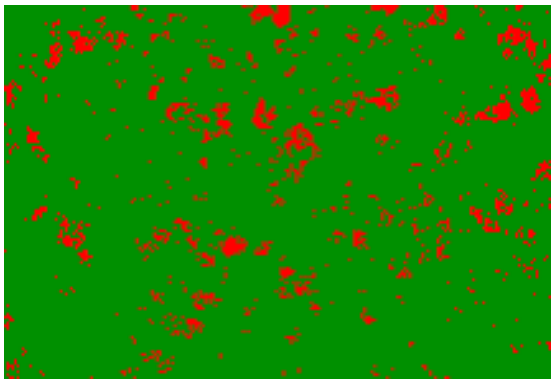

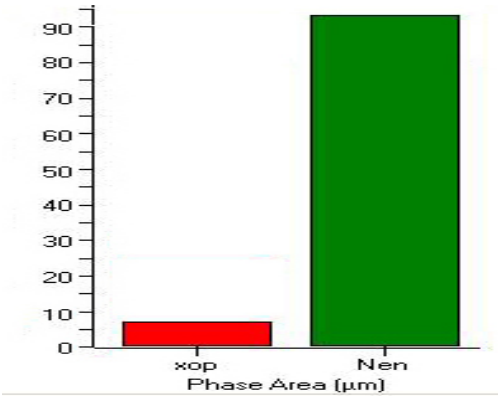

a) Sample 6 (MS: 120), x200

b) γ_{p6} = 7,765 %

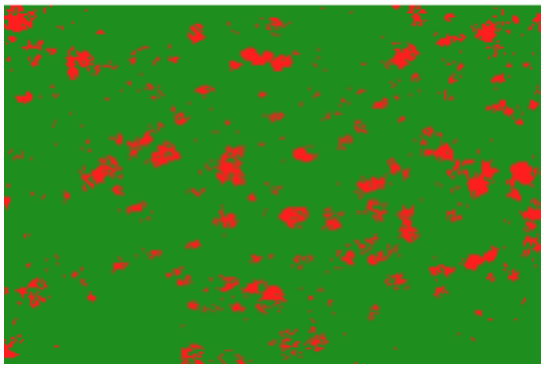

c) Sample 7 (MS: 200), x200

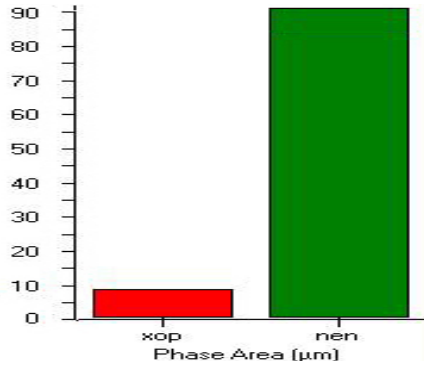

d) γ_{p7} = 8,125 %

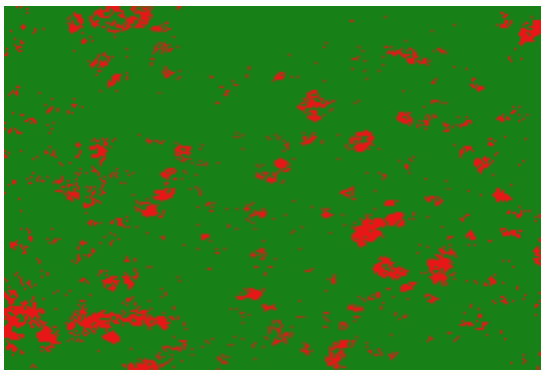

e) Sample 8 (MS: 210), x200

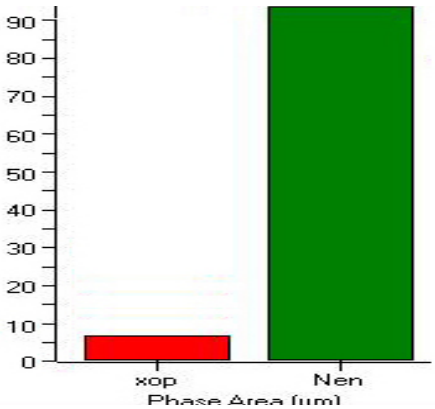

f) γ_{p8} = 7,773 %

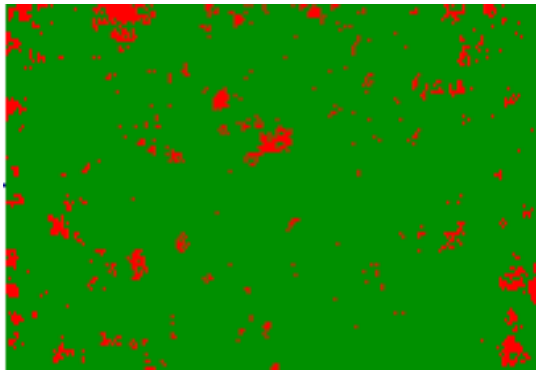

g) Sample 9 (MS: 220), x200

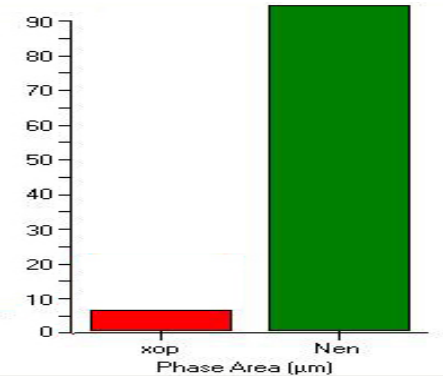

h) γ_{p9} = 7,321 %

Figure 3. Image of microstructure (a) and plasma coating porosity chart Al2O3 – TiO2 (b) depends on Lp; Ip and Gp

Analysis of microscopic organization images and visual 2D graphics of the porosity of Al2O3 – TiO2 plasma coating material (denoted in red) on Figure 2. and Figure 3.

Experimental sample groups No. 01; 02 and 03 (Fig. 2, a ÷ f) have average porosity decreasing from (01 = 14.52 %) to (03 = 11.355 %). It is happened due to the increased current of plasma as a favorable condition for better particle melting when they collided on the substrate, decreasing the porosity. The observation is in conformity with the investigations

of other researchers [14]-[16]. The characteristic properties of the plasma coating micromaterial organization on these 3 samples have many regions of porous structure of different sizes, distributed relatively evenly over the entire survey surface. However, these test samples have a large porosity of the coating material, so it is necessary to apply more solutions to introduce the penetrated substance to reduce porosity and, at the same time, increase the load resistance and resistance to mechanical wear and chemical corrosion compared to the post-spray coating state.

Experimental sample groups No. 04, 05 (Figure 2, g) and No. 06 (Figure 3, a, b) have significantly reduced the average porosity of the coating from (04 = 10.985%) to (06 = 7.765%) compared to samples No. 01, 02, and 03 above. The ceramic particles flying with a slight increase in spraying distance provided more delayed time and improved the melting condition. In this context, the increased plasma current means more thermal energy for the particle stream. That is why the porosity in the coating is less than sample groups No. 1, 2, and 3. The plasma coating micromaterial organization has sub-regions of porous structure formed after spraying with finer, smaller sizes, more evenly distributed according to the surface of the survey sample **Error! Not a valid bookmark self-reference.** - [22] . That proves that they have quite good material structural properties; if the affected substance is introduced into the coating, it will have a higher performance under mechanical wear loads.

Sample Group Nos. 07, 08, and 09 (Figure 3, c- g) are micrologically organized with almost the same basic characteristics as Form Nos. 04, 05, and 06, respectively. The ceramic material is not well thermally conducted, and the further fly time in the plasma stream encouraged the favorable melting state of the feedstock material before the collision on the substrate. These three samples had average porosity in the range (07 = 8.125) ÷ (09 = 7.321%), down very much from the 6 samples considered above. This index is much less than the same one (12–14% porosity) announced in [8], where the spraying distance is 100 mm. However, here, although the subregions of the porous structure are fairly evenly distributed on the surface of the samples, they are not very smooth in size. It is useful to mention the different roles of porosity, especially when dealing with the ceramic system of the material. On one side, the porosity helps to increase the cohesion in the coating, which increases the wear resistance of the surface. But the size and arrangement of the porosity in the thermal insolation coating are the positive conditions.

4. Conclusion

The results of analysis of microscopic organization images and 2D diagrams on optical microscopes with built-in Image Pro-Analyzer software show that the average porosity of the Al2O3-TiO2 plasma coating shows that there is a law of inverse decrease in the increasing direction of the distance: spray in the range Lp = 100–200 mm, increase proportional to the increase of the current plasma flow rate in the range Ip = 400–600 A, provided that the powder feed flow Gp = 1.7 kg/h and the injection rate Vp = 50 mm/min. The degree of influence of the three main technological parameters (Lp, Ip, and Gp) in the survey limit domain may be due to the selected Lp spray distance within the relatively wide recommended range of the plasma injection equipment supplier. In addition, when spraying with Ip parameters selected at advanced levels, it also contributes to favorable

conditions for the formation of plasma coatings whose structure distributes pores more evenly or is improved.

Al2O3-TiO2 plasma coating after direct spraying on the surface of SS400 steel plate samples according to selected L9 orthogonal experimental planning regimes is still quite high, not satisfactory as desired. Therefore, in further experimental planning studies of the L27 type, it is necessary to adjust the value domain of the input technology parameters in order to minimize the porosity of the plasma coating to the smallest level and improve its working performance. However, it should be emphasized that, in general, according to technological principles, it is impossible to get a coating without pores inside it using any known basic thermal coating method.

Acknowledgement

This research has not received external funding.

References

[1] J. Pan, Y. Zheng, Y. Zheng, W. Ye, W. Yu, "Solidification mechanismand microstructure evolution of Al2O3-ZrO2 ceramic coating prepared by combustion synthesis and thermal explosion spraying", Ceramic International,43(5),4034-4041,2017, doi: 10.1016/j.ceramint.2016.11.153

[2] I. V. Blinkov, D. S. Belov, A I Laptev, A. S. Anikeev and V. V. Ivanov, "Flame sprayed and plasma sprayed Al2O3-TiO2 coatings", J. Phys.: Conf. Ser. 1954 012003, 15th International Conference on Films and Coatings (ICFC 2021), doi:10.1088/1742-6596/1954/1/012003

[3] K. Yang, J. Li, Q. Wang, Z. Li, Y. Jiang, Y. Bao," Effect of laser remelting on microstructure and wear resistance of plasma sprayed Al2O3- 40%TiO2 coating", Wear, vol 426-427, Part A,314-318, doi: 10.1016/j.wear.2019.01.100

[4] Y. Lu, Y. Peng, Z. Shi," Plasma sprayed Al2O3–40%TiO2 coating by laser remelting: Structural evolution, tribological properties and DFT calculation", Tribology International, vol 189,109009,2023, doi: 10.1016/j.triboint.2023.109009

[5] G. M. T. Basha, A. Srikanth, B. Venkateshwarlu," A Critical Review on Nano structured Coatings for Alumina-Titania (Al2O3-TiO2) Deposited by Air Plasma Spraying Process (APS)", Materialstoday: Proceedings,22(4), 1554-1562,2020, doi: 10.1016/j.matpr.2020.02.117

[6] W. T. Urmi, M.M. Rahman, W.A.W. Hamzah," An experimental investigation on the thermophysical properties of 40% ethylene glycol based TiO2-Al2O3 hybrid nanofluids", International Communication in Heat and Mass Transfer,116,104663,2020, doi: 10.1016/j.icheatmasstransfer.2020.104663

[7] A. Richter, L. M. Berger, Y. J. Sohn, S. Conze, K. Sempf, R. Vaßen, "Impact of Al2O3-40 wt.% TiO2 feedstock powder characteristics on the sprayability, microstructure and mechanical properties of plasma sprayed coatings", Journal of European Ceramic Society,39(16),5391-5402,2019, doi: 10.1016/j.jeurceramsoc.2019.08.026

[8] M. Michalak, L. Latka, P. Sokolowski, Rolando T. Candidato & Andrzej Ambroziak,

"Effect of TiO2 on the microstructure and phase composition of Al2O3 – TiO2 APS sprayed coatings", Bulletine of the Polish Academy of Sciences, Technical Sciences, 69(2), 2021, doi:10.24425/bpasts.2021.136735

[9] Material Product Data Sheet Aluminum Oxide 40% Titanium Dioxide Powders, Oerlikon Metco, 2022.

[10] Material Product Data Sheet Aluminum Oxide 13 % Titanium Dioxide Powders, Oerlikon Metco, 2020.

[11] TS1380 Aluminum Oxide and 3 % Titanium Dioxide Powders.Standford Advance Material. https://www.sputtertargets.net/aluminum-oxide-and-3-titanium-oxide-powder

[12] J. J. Zhang, Z. H. Wang, P. H. Lin, L. Q. Si, G. J. Shen, Z. H. Zhou, S. Q. Jiang and W. H. Lu "Corrosion of plasma sprayed NiCrAl / Al2O3 – 13% TiO2 coatings with and without sealing", Surface Engineering,2012, Vol. 28, No 5, doi :10.1179/1743294412Y.0000000004

[13] M. Michalak, L. Łatka, P. Sokołowski, A. Niemiec and A. Ambroziak," The Microstructure and Selected Mechanical Properties of Al2O3 + 13 wt % TiO2 Plasma Sprayed Coatings", Coatings,10(2),173,2020, doi: 10.3390/coatings10020173

[14] J. Antoš, K. Lencová and A. Keslová, " Influence of processing parameters and heat input level on the functional properties of atmospheric plasma sprayed Al2O3-3TiO2 commercial coating", IOP Conference Series Materials Science and Engineering 1178(1):012003, doi:10.1088/1757-899X/1178/1/012003

[15] A. R. M. Sahaba, N. H. Saadb, S. Kasolangb, and J. Saedonb," Impact of Plasma Spray Variables Parameters on Mechanical and Wear Behaviour of Plasma Sprayed Al2O3 3%wt TiO2 Coating in Abrasion and Erosion Application", International Symposium on Robotics and Intelligent Sensors 2012 (IRIS 2012), Procedia Engineering, 41(2012),1689-1695, doi: 10.1016/j.proeng.2012.07.369

[16] T. D. Duy, V. Duong," A New Solusion to Save Production Cost in the Deposition of the Wear-Resistant Coating", Chapter in eBook "Coating for High-Temperature Environment ", Editors: A. Pakseresh &K. K Amirtharaj Mosas, Springer Nature, pp.126-160, 2024, doi: 10.1007/978-3-031-45534-6_6

Error! Not a valid bookmark self-reference. R. Yılmaz, A. O. Kurt, A. Demir, and Z. Tatlı, "Effects of TiO2 on the mechanical properties of the Al2O3–TiO2 plasma sprayed coating," Journal of the European Ceramic Society, vol. 27, no. 2–3, pp. 1319–1323, 2007, doi: 10.1016/j.jeurceramsoc.2006.04.099

[18] T. S. Rajesh and R. V. Rao, "Experimental Investigation and Parameter Optimization of Al2O3-40% TiO2 Atmospheric Plasma Spray Coating on SS316 Steel Substrate," Materials Today: Proceedings, vol. 5, no. 2, pp. 5012–5020, Jan. 2018, doi: 10.1016/j.matpr.2017.12.079

[19] P. Kazimierczak and A. Przekora, "Osteoconductive and Osteoinductive Surface Modifications of Biomaterials for Bone Regeneration: A Concise Review," Coatings, vol. 10, no. 10, p. 971, 2020, doi: 10.3390/coatings10100971

[20] R. J. K. Wood and P. Lu, "Coatings and Surface Modification of Alloys for Tribo-Corrosion Applications," Coatings, vol. 14, no. 1, p. 99, 2024, doi: 10.3390/coatings14010099

[21] A. Thakur, A. Kumar, S. Kaya, R. Marzouki, F. Zhang, and L. Guo, "Recent Advancements in Surface Modification, Characterization and Functionalization for Enhancing the Biocompatibility and Corrosion Resistance of Biomedical Implants," Coatings, vol. 12, no. 10, p. 1459, 2022, doi: 10.3390/coatings12101459

[22] Q. Zheng, Y. Li, C. Ma, J. Sun, Y. Gao, and L. Feng, "Investigation on Al-Al2O3 refractories with Al2O3-Ti2O3 raw material at evaluate temperatures," Journal of the European Ceramic Society, vol. 44, no. 2, pp. 1289–1295, Feb. 2024, doi: 10.1016/j.jeurceramsoc.2023.10.006